SLOPE: A two-part method for the enrichment of ring stage *Plasmodium falciparum* parasites

Audrey C. Brown, Jennifer L. Guler
Department of Biology, University of Virginia, Charlottesville, VA.

Abstract

The growing threat of antimalarial resistance highlights the need for continued study of *Plasmodium falciparum*, the deadliest of the human-infective malaria parasites. The majority of antimalarial drugs target the blood stages of the *P. falciparum* lifecycle, including early ring-infected erythrocytes. Given the discovery of a ring stage-specific quiescence phenotype, this stage is particularly important in the context of resistance. However, many studies have focused on late, more mature, blood stages due to efficient culture enrichment methods that take advantage of density differences or the accumulation of a paramagnetic pigment. Furthermore, the lack of enrichment methods for ring stage parasite results in considerable host contamination, which limits the success of sensitive downstream analyses such as metabolomics. Here, we present a method for the rapid enrichment of *P. falciparum* cultures that effectively enriches ring-infected erythrocytes. Our method utilizes the lytic agent streptolysin-O (SLO) to preferentially lysed uninfected erythrocytes. The remaining material is rich in intact infected erythrocytes and can be efficiently separated from lysed erythrocyte membranes using Percoll gradient centrifugation. We demonstrate that our SLO-Percoll (SLOPE) method is capable of enriching ring-infected erythrocyte density by over 20-fold, regardless of the culture media or parasite line. Additionally, we show that enriched parasites remain viable after this treatment. SLOPE enrichment is scalable, rapid (30min), and non-toxic making it ideal for use upstream of a variety of sensitive analyses.

Introduction

Malaria, caused by protozoan parasites of the *Plasmodium* genus, is a continuing threat to global health. While five *Plasmodium* species cause malaria in humans, *Plasmodium falciparum* is responsible for the large majority of malaria mortality (1). The majority of clinically used antimalarial drugs, including artemisinin (ART), target the asexual blood stages of the parasite lifecycle (including rings, trophozoites, and schizonts) (2). The current World Health Organization recommendation for treatment of malaria is ART combination therapy (3). However, clinical resistance has now been reported to both ART and almost all of its partner drugs (4-6). The emergence and spread of resistance to these drugs threatens to undo the progress made in malaria mortality reduction and emphasizes the dire need to understand and combat parasite drug resistance.

Omics-based studies have gained popularity in recent years for the characterization of biological phenomenon, such as drug resistance. Genomics, transcriptomics, and proteomics rely on the identification of DNA, RNA, or amino acids, respectively, in order to provide novel insights into biological questions. These biological molecules ultimately form genes, transcripts, and proteins that serve to regulate cellular activity. By directly measuring the products of cellular activity, metabolomics allows interpretation of many pathways without functional knowledge of the genes, transcripts, or proteins that underlie a phenotype. The *P. falciparum* genome is poorly annotated (40% of genes) compared to many model organisms (85% of genes for *S. cerevisiae*), making metabolomics an attractive method for unbiased study of parasite biology (7, 8). Indeed, *Plasmodium* metabolomics has become increasingly popular in recent years for investigation of parasite biology and antimalarial drug action (9-18).

The large majority of asexual *P. falciparum* metabolomics studies to date have been performed on late stage (trophozoites and schizont) parasite samples. This is due in part to the larger biomass of late stage parasites but is also due to the availability of effective late stage parasite enrichment methods; erythrocytes infected with late stage parasites can be enriched by magnetic purification due to the paramagnetic properties of hemozoin, which accumulates as the parasite matures. Importantly, there is currently no method for enrichment of the early form of the parasite (ring stage) (19). However, ring stage-specific ART-induced quiescence has highlighted the requirement for an effective method for ring stage isolation and study (20).

We previously explored parameters important for metabolomics studies of *P. falciparum* (21). Not surprisingly, the metabolomes of non-enriched ring stage samples were heavily influenced by host erythrocyte contamination (about a third of 375 total metabolites detected were associated with the blood cells used for parasite propagation). A recent multi-omics study also noted poor coverage and high levels of variability in ring stage proteome (18). Results from these two studies emphasize the introduction of ‘noise’ from a large excess of human host

erythrocyte material present in ring stage samples; without an effective way to separate infected from uninfected erythrocytes, only a small fraction of the total cells contain ring-stage parasites (typical parasitemia ranges between 1%-10%). The challenge of detecting parasite-specific material is further exacerbated by leftover erythrocyte membrane material following commonly used lysis steps (21). Data analysis steps (i.e. normalization of metabolomics samples) were not sufficient to correct for this heavy host contribution {Carey, 2018 #383}, thus necessitating improvements in upstream purification steps.

In this study, we present a method for the enrichment of viable ring stage *P. falciparum* infected erythrocytes that is both rapid and non-toxic. Additionally, this method can be scaled to the needs of individual experiments without compromising these attributes.
The effective removal of host erythrocyte material is shown to be unaffected by parasite line or culture media further highlighting utility for a range of experimental needs. This is the first published enrichment method which effectively enriches ring stage parasites to increase parasitemia and reduce host erythrocyte contamination.

Results

Enrichment of ring-infected erythrocytes
We developed an SLO–Percoll (SLOPE)-based protocol for the enrichment of ring stage *P. falciparum* infected erythrocytes (**Fig 1,** see *Materials and Methods* for details). SLO is a pore forming toxin that has been found to preferentially lyse uninfected erythrocytes, leaving the large majority of infected erythrocytes intact (22). Using the protocol outlined by Jackson, *et al*. with slight modifications, we were able to achieve comparable levels of discrimination in lysis of erythrocytes populations (93.4% and 9.9% lysis of uninfected and infected erythrocytes, respectively, **Fig. 2A** and **B,** yellow highlight). In addition to reproducing lysis levels shown by Jackson, *et al*., we quantified uninfected and infected erythrocyte lysis across a gradient of SLO concentrations. More complete lysis of uninfected cells (>99%) was obtained at the cost of greater infected erythrocyte lysis by increasing SLO quantity. For example, we found that 47U of SLO leads to >99% lysis of uninfected erythrocytes and 40% lysis of infected erythrocytes (**Fig. 2A** and **B,** grey highlight). Additionally, we show that SLO favors uninfected erythrocyte lysis irrespective of parasite line or culture media. SLO shows comparable lysis discrimination between uninfected and infected erythrocytes in parasites grown in RPMI 1640 supplemented with Albumax II or RPMI 1640 supplemented with 20% human serum (**Fig. 2A**, maximum discrimination between uninfected and infected erythrocytes: Albumax supplementation = 83.5%; serum supplementation = 81.6%). SLO lysis shows considerable discrimination between uninfected and infected erythrocytes across all three lines tested (**Fig. 2B**).

After treatment with SLO, parasite samples contain a mixture of primarily lysed erythrocyte membranes (from uninfected erythrocyte lysis), termed ghosts, and intact erythrocytes (enriched in infected erythrocytes) (**Fig. 1B**). For the second part of the enrichment protocol, we exploited the difference in density of intact erythrocytes and ghost membranes to separate the two populations. We found that intact erythrocytes travel through a 60% Percoll gradient during centrifugation while erythrocyte ghosts remain above the Percoll layer (**Fig. 1D**, see below). Collection of the intact erythrocyte population leads to a sample with up to greater than 20-fold increase in the parasite to erythrocyte membrane ratio. In one representative trial, we demonstrate enrichment of ring stage samples to a final parasitemia over 80% (22-fold increase over starting parasitemia, **Fig. 2C**). Higher levels of enrichment are attainable with higher amounts of SLO (up to 48-fold with 55 units of SLO, **Fig. 2D**) but this is at the cost of parasite material (up to ~40% of infected erythrocytes, **Fig. 2A and B**).

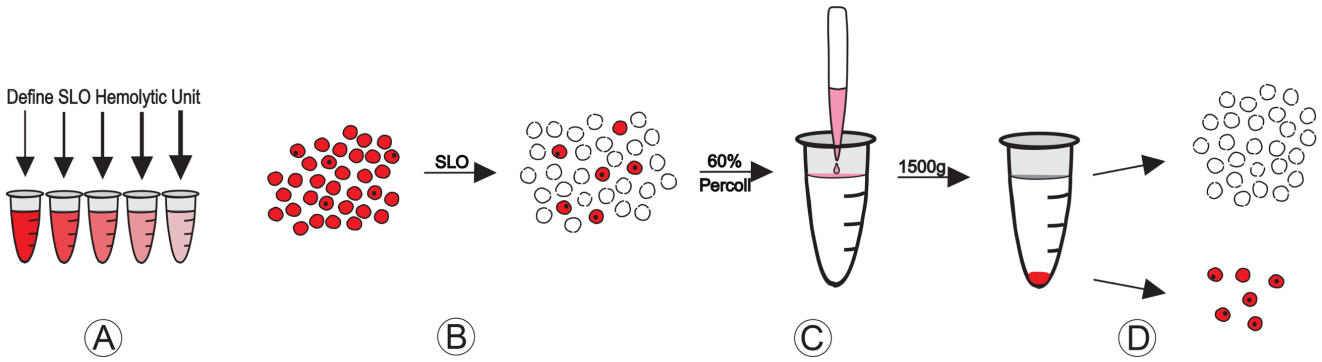

Figure 1. SLOPE enrichment overview. (A) Hemolytic activity of SLO is assessed on uninfected erythrocytes to define a unit (the amount of SLO necessary for 50% lysis of 50µl uninfected erythrocytes at 2% hematocrit in PBS for 30 min at 37°C). (B) Synchronized cultures are treated with a defined quantity of SLO units to preferentially lyse uninfected erythrocytes. (C) SLO treated samples are layered over a 60% Percoll gradient and centrifuged at 1500xg to separate lysed ghosts from intact cells. (D) The upper layer of Percoll containing lysed ghosts is discarded while the lower, intact, infected erythrocytes enriched fraction is collected.

We performed SLOPE on mixed stage populations to determine whether our protocol biases enrichment of certain asexual stages. We found that SLOPE enrichment of lightly synchronized cultures (i.e. contains rings and some early trophozoites) did not result in any alteration of the ring to trophozoite proportion (**Fig. S1A**). SLOPE enrichment was also unbiased when performed on completely asynchronous cultures (includes rings, trophozoites, and schizonts). However, the protocol did result in a non-significant drop in schizont percentage (**Fig. S1B**). Centrifugation and washes likely lysed fragile schizont-infected erythrocytes resulting in partial loss of the schizont population.

Next, we employed immunofluorescence detection of erythrocyte components to confirm that Percoll gradient density centrifugation removes ghost erythrocyte membranes from SLO treated samples (**Fig. 1D**). Specifically, we visualized all erythrocyte membranes through detection of an erythrocyte surface protein (CD235a); we identified ghosts through detection of

an intra-erythrocyte protein (spectrin). Untreated (control) samples contain high erythrocyte membrane to parasite ratios (~100:1 due to ~1% parasitemia) as expected, and almost all membranes (>99%) are in the form of intact cells (spectrin negative, **Fig. 3A** and **B**). All erythrocyte membranes in samples treated with a nondiscriminatory lytic agent (saponin) are lysed ghosts (spectrin positive); however, the same high erythrocyte membrane to parasite

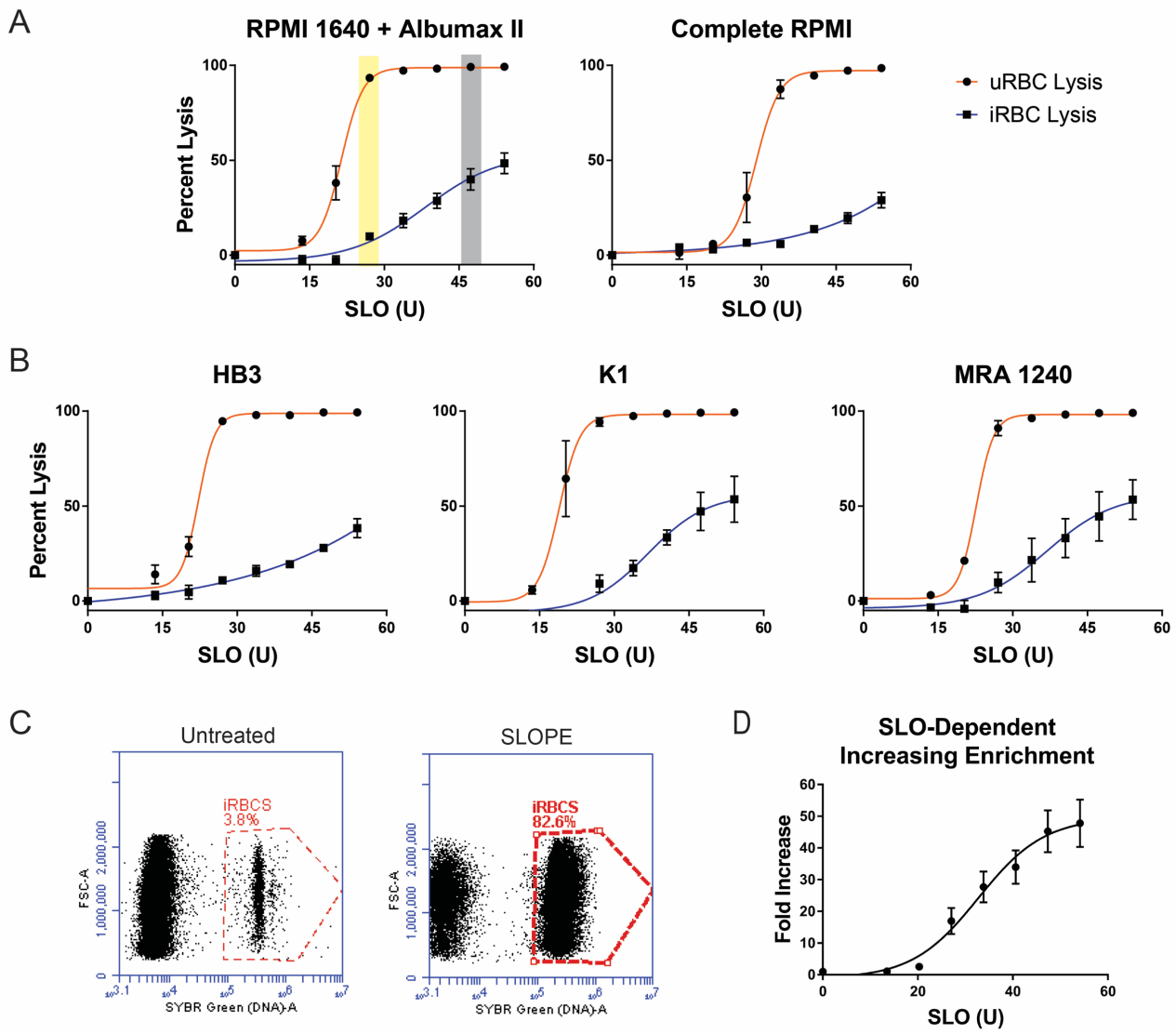

Figure 2. SLOPE enriches ring stage *P. falciparum* irrespective of parasite media or line. (A) SLO lysis of uninfected and infected erythrocytes in parasites grown in RPMI 1640 supplemented with Albumax II (N = 9; Error bars represent SEM) or RPMI 1640 supplemented with 20% human serum (N = 6; Error bars represent SEM). (B) Two common laboratory adapted *P. falciparum* strains (HB3 and K1) and one more recently laboratory adapted field isolate (MRA-1240) were SLOPE enriched (N = 3 per line, Error bars represent SEM). (C) SYBR-Green based flow cytometry measurements before and after SLOPE enrichment. Flow plot shows single cells within the erythrocyte size range. The infected erythrocyte fraction ("iRBCs") is denoted within dashed red gate. (D) Parasitemia fold increase upon treatment with increasing SLO units relative to untreated controls. Represented samples were grown in RPMI 1640 supplemented with Albumax II (N = 9; bars represent SEM).

ratio (100:1) that is observed in control samples persists. In samples treated only with SLO (no Percoll gradient centrifugation), a subset of cells enriched for infected erythrocytes remains intact (1 of 4 erythrocytes in **Fig. 3A**). However, the considerable lysed erythrocyte population remains, leaving the erythrocyte membrane to parasite ratio at 100:1. Complete SLOPE enrichment demonstrates the effectiveness of Percoll centrifugation for separating ghosts and intact cells by removing this lysed erythrocyte population, leaving a >99% intact erythrocyte population that is enriched for parasites (25-fold decrease in the erythrocyte membrane to parasite ratio; starting of 100:1, final of 4:1)**.** Image quantification revealed that <0.2% of erythrocytes in SLOPE enriched samples were ghosts (**Fig. 3B**).

Measurement of parasite viability after SLOPE enrichment

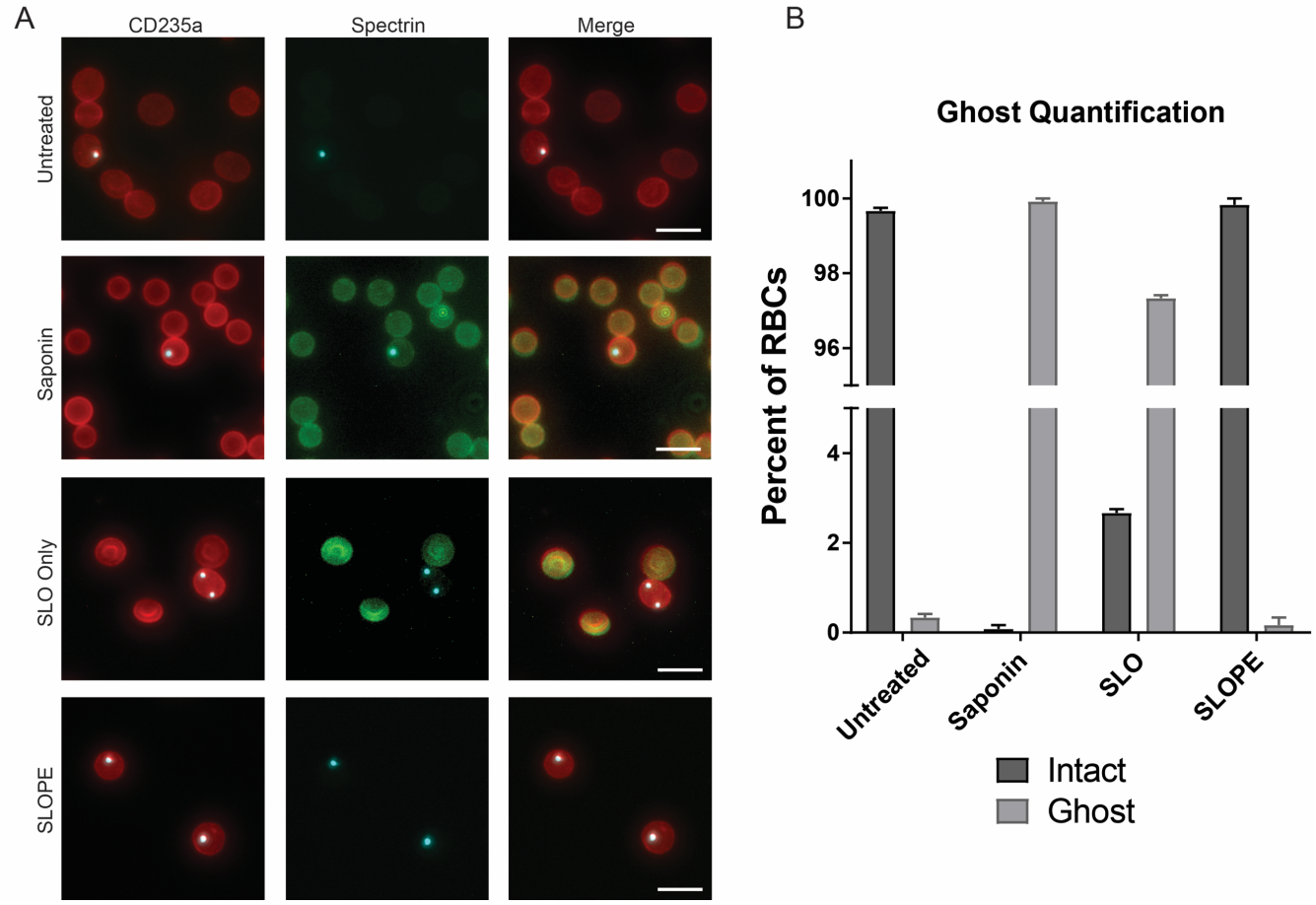

Figure 3. Validation of ghost separation from intact erythrocytes by Percoll step for SLOPE. (A) Intact erythrocytes are shown as CD235a (red) positive and spectrin (green) negative. Lysed erythrocytes, termed ghosts, are shown as CD235a and spectrin double positive (yellow in merge). All images show parasites stained with SYBR Green (cyan). 40X Magnification; bar represents 10um. Saponin samples were treated with 0.15% saponin for 5 minutes. SLO samples were treated with 40U of SLO for 6 minutes but were not centrifuged through a Percoll gradient. SLOPE samples were also treated with 40U SLO but were subjected to Percoll gradient centrifugation (B) Proportions of lysed ghosts and intact erythrocytes quantified from fluorescence microscopy imaging across different treatments using SYBR Green dye and CD235a and spectrin antibodies (*N* = 3; 400 erythrocytes per condition per preparation, error bars represent SEM).

We sought to test the effect of SLOPE enrichment on parasite metabolism and viability. First, parasites were stained with a mitochondrial membrane potential dependent dye to determine the fraction of metabolically active parasites (**Fig. 4A**). The percentage of parasites with an active mitochondrial membrane potential was not significantly different between SLOPE enriched samples and untreated controls (*untreated*=97%, *SLOPE*=94%, *p*=0.36, **Fig. 4A**). To assess parasite viability on a longer-term scale, we monitored parasite growth following SLOPE enrichment. This was accomplished by diluting SLOPE enriched parasites with fresh erythrocytes to reduce parasitemia to appropriate levels for culture (<5%). When compared to that of non-enriched control flasks, the growth rate of parasites from SLOPE enriched samples showed no apparent growth defects over the time period measured (96h) (**Fig. 4B**). Ring stage parasites retain normal morphology following SLOPE enrichment further providing evidence that SLOPE enrichment does not damage parasites (**Fig. 4C**).

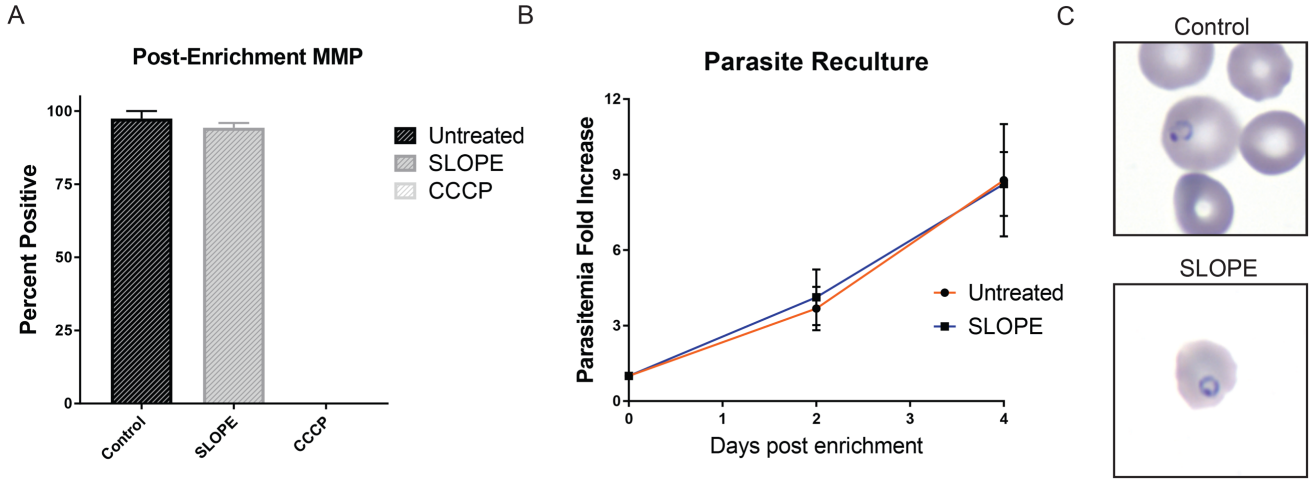

Figure 4. SLOPE enriched parasites remain viable. (A) $DiIC_1(5)$ MMP measurements obtained by flow cytometry in untreated and SLOPE enriched parasites (p = 0.36, N = 3, error bars represent SEM). (B) 96h growth rate of parasites from untreated controls or SLOPE enriched samples diluted with uninfected erythrocytes (N = 4, error bars represent SEM). (C) Ring stage infected erythrocytes visualized by Giemsa-stain at 100X magnification.

Discussion

Here, we introduce a method for achieving considerable ring stage parasite enrichment that is effective across various *P. falciparum* lines and culture media (**Fig. 1**; **Fig. 2A-B**). Our two-part SLOPE enrichment protocol utilizes the preferential lysis of uninfected erythrocytes by SLO to create density differences between a parasite-rich intact population and a ghost population derived from primarily uninfected erythrocyte lysis. Centrifugation through a Percoll gradient readily separates these two populations leading to the collection of an intact erythrocyte fraction enriched by over 20-fold (**Fig. 2C-D**). We confirm that unlike the use of a lytic agent

alone, complete SLOPE enrichment effectively removes lysed ghosts thereby greatly reducing the erythrocyte to parasite ratio in ring stage samples (**Fig. 3**).

The SLOPE method has several advantages for isolation of material to be used for sensitive downstream analyses. Firstly, our method can be performed rapidly (~30-40 min). This is equal to or faster than the amount of time needed to perform the field-accepted purification method for isolation of late stage parasites by magnetic column purification (~30min to 1hr). Rapid purification ensures the cellular state of samples is as close as possible to the true culture phenotype, which is important for sensitive downstream analyses such as metabolomics. Secondly, this method is highly scalable and can be used on culture amounts that range from a fraction of a milliliter to combined pools of many flasks (tens to hundreds of milliliters). Finally, our method allows parasites to remain inside host erythrocytes, which likely minimizes artifacts cellular stress. Our studies confirm that parasites remain metabolically healthy after SLOPE enrichment through both short-term (MMP measurements) and long-term (re-culture growth rate) viability assays (**Fig. 4**). One caveat of this method may be the cost of SLO lytic agent. Researchers seeking to regularly enrich large quantities of parasites may consider in-house isolation of SLO from *Streptococcus pyogenes* culture in place of purchasing commercially available SLO. An additional caveat of SLOPE enrichment is the loss of parasite material. However, due to the scalability of this method, starting material can be increased to compensate for this loss. When sample material is limited, researchers may wish to use lower quantities of SLO to minimize lysis of infected erythrocytes.

The inability to enrich for ring stage parasites has exacerbated host contamination of samples and limited our ability to discern interesting parasites phenotypes (18, 21). Successful ring stage enrichment will beneficially reduce contribution of non-parasite factors not only for metabolomics studies, but for a variety of ring stage related experiments. For example, reduction of erythrocyte material may benefit the isolation of ring stage organelles, capture of rare events (e.g. sub-microscopic level infection), and reduction of human DNA and RNA prior to sequencing. With SLOPE enrichment as a tool, researchers can more accurately study the ring stage of the *P. falciparum* erythrocytic cycle.
Improvements in our understanding of parasite biology will lead to more effective treatments for this deadly disease.

Methods

Parasite Cultures

P. falciparum cultures were maintained with human erythrocytes at 3% hematocrit in RPMI 1640 HEPES (Sigma Aldrich, St Louis, MO) supplemented with either 0.5% Albmumax II Lipid-Rich BSA (Sigma Aldrich, St Louis, MO) and 50 mg/L hypoxanthine (Thermo Fisher Scientific, Waltham, MA) or with 20% human serum (Valley Biomedical, Winchester, VA). Cultures were

grown at 37°C under 5% oxygen, 5% carbon dioxide, 90% nitrogen gas (26). Dilution of cultures with uninfected erythrocytes to maintain parasitemia at <5% was performed every other day as was changing of culture medium. Parasitemia was determined by flow cytometry using SYBR-Green staining (27). Cultures were confirmed negative for mycoplasma monthly using a LookOut Mycoplasma PCR detection kit (Sigma Aldrich, St Louis, MO).

SLO activation and storage

Streptolyisn-O (SLO) activation was performed as previously described (Jackson 2007). Following activation, SLO was stored in aliquots at -20 °C until shortly before use. Hemolytic units (U) of each SLO batch was quantified from a stored aliquot; one unit equals the amount of SLO necessary for 50% lysis of 50µl uninfected erythrocytes at 2% hematocrit in PBS for 30 min at 37°C. Hemolytic activity was recurrently assessed (approximately monthly) in triplicate to control for SLO degradation over time.

SLOPE enrichment

P. falciparum cultures were synchronized to the ring stage prior to enrichment using 5% D-sorbitol (Sigma Aldrich, St Louis, MO) (28). SLO lysis was performed as previously described but with modifications (22) (**Fig. 1; Text S1**). Briefly, erythrocyte density was measured using a Cellometer Auto T4 (Nexcelom Biosciences, Lawrence, MA). Cell density was adjusted to $2x10^9$ erythrocytes/ml. The desired amount of SLO (between 0U and 55U) was added in a ratio of 2 parts SLO solution to 5 parts erythrocytes. Samples were mixed well by pipetting and incubated at room temperature for 6 min. 5-10 volumes of 1X PBS or media (RPMI 1640 HEPES) were added and cells were centrifuged at 2,500xg for 3 min. After removal of the supernatant, cells were washed twice more with 1X PBS or media. Following SLO lysis, cells suspended in 1X PBS were layered onto a 60% Percoll gradient (Sigma Aldrich, St Louis, MO) and centrifuged at 1,500xg for 5-10 min depending on the volume of the gradient. The top layer of Percoll was discarded while the lower cell pellet was collected and washed twice with 1X PBS or media.

SLO lysis curves

Cells were treated with varying amounts of SLO as described above. Flow cytometry was used to assess total erythrocyte density (gated for intact erythrocytes) and infected erythrocyte density (gated for SYBR-Green positive intact erythrocytes) on a BD Acurri C6 flow-cytometer (BD Biosciences, San Jose, CA). Infected erythrocyte density was subtracted from total erythrocytes to determine uninfected erythrocyte density. Percent lysis of uninfected and infected erythrocyte populations were determined relative to an untreated control.

Re-culturing of SLOPE enriched parasites

P. falciparum cultures were synchronized using 5% D-sorbitol immediately prior to use. The synchronized culture was split to <1% parasitemia to generate an untreated control flask, while

the remaining 9 mL of culture were enriched according to the SLOPE protocol described above. Following enrichment, parasite density of was measured by SYBR-Green based flow cytometry and a “SLOPE” flask was seeded with the amount of the enriched cells necessary to match the parasite density of the respective untreated control flask. Uninfected erythrocytes were added to the SLOPE flask to bring hematocrit up to 3%. Parasitemia of flasks was measured every 48h for 2 replication cycles.

Mitochondrial membrane potential measurements

Mitochondrial membrane potential (MMP) was assessed using the MitoProbe DiIC1(5) kit (Thermo Fisher Scientific, Waltham, MA). DiIC1(5) accumulates in eukaryotic mitochondria in a mitochondrial membrane potential-dependent manner (29). The effect of SLOPE enrichment on MMP was tested using ring stage synchronized cultures of MRA1240 (BEI Resources, NIAID, NIH: *Plasmodium falciparum*, Strain IPC 1502/MRA-1240, contributed by Didier Ménard). Following SLOPE enrichment, parasites were incubated with 50nM DiIC1(5) in media at $1x10^6$ parasites/mL for 30 min at 37°C. Negative controls treated with the oxidative phosphorylation uncoupler, Carbonyl cyanide m-chlorophenyl hydrazone (CCCP) (Thermo Fisher Scientific, Waltham, MA). Untreated positive controls and were assayed alongside enriched samples. Samples were co-stained with SYBR Green and analyzed using 488nm (for SYBR) and 640nm (for DiIC1(5)) filters on a BD Accuri C6 flow cytometer. The percentage of MMP positive parasites was determined as the ratio of DiIC1(5) positive to SYBR Green positive events. Significance between treatment and control groups was calculated in Graphpad Prism using an unpaired t-test.

Microscopy

Slides for brightfield imaging were prepared by fixation in methanol for 1 minute prior to the addition of Giemsa stain for 15 minutes (Sigma Aldrich, St Louis, MO). Brightfield images were obtained on an Eclipse Ci microscope (Nikon, Melville, NY) using and ImagingSource microscope camera and NIS Elements Imaging Software (Nikon, Melville, NY). For parasite stage quantification, slides were prepared for brightfield microscopy as described above both prior to and after SLOPE enrichment. Parasites were categorized by eye as either a ring, trophozoite, or schizont. In the case of a multiply-infected erythrocytes, all parasites were counted separately. Gametocytes were excluded from counting.

CD235a is constitutively present on the erythrocyte outer surface and thus, both intact erythrocytes and lysed ghosts are CD235a+. Conversely, spectrin is located in the erythrocyte cytoskeleton meaning anti-spectrin cannot access the antibody target in intact erythrocytes. However, pores in lysed erythrocyte membranes (saponin or SLO treated) allow passage of antibodies into the erythrocyte cytosolic compartment making these cells spectrin+. For fluorescent imaging, unfixed samples (average parasitemia of 1%) were blocked with 2% BSA followed by staining in suspension with a 1:100 dilution of mouse anti-alpha I spectrin antibody

(Abcam, Cambridge, MA) at $2x10^7$ erythrocytes/ml. Samples were washed then incubated with the fluorescently conjugated secondary antibody, goat anti-mouse Alexa Fluor 594 (Abcam, Cambridge, MA) at 1:1000 dilution. Following additional washes, samples were incubated with the fluorescently conjugated CD235a-PE antibody (Thermo Fisher Scientific, Waltham, MA) at 1:100, and SYBR Green (Thermo Fisher Scientific, Waltham, MA) at 1:10,000. A wet mount was prepared on microscope slides, and samples were immediately imaged. Images were acquired on an EVOS FL Cell Imaging System (Thermo Fisher Scientific, Waltham, MA) using RFP, GFP, and Texas Red excitation and emission settings.

Acknowledgements
Special thanks to Michelle Warthan for culturing support. ACB is supported by an institutional training grant (5T32GM008136-33).

References

1. WHO. 2017. World Malaria Report. Organization WH, Geneva, Switzerland.
2. Haldar K, Bhattacharjee S, Safeukui I. 2018. Drug resistance in Plasmodium. Nature Reviews Microbiology 16:156.
3. WHO. 2015. Guidelines for the treatment of malaria. Geneva, Switzerland.
4. Blasco B, Leroy D, Fidock DA. 2017. Antimalarial drug resistance: linking Plasmodium falciparum parasite biology to the clinic. Nat Med 23:917-928.
5. Dondorp AM, Nosten F, Yi P, Das D, Phyo AP, Tarning J, Lwin KM, Ariey F, Hanpithakpong W, Lee SJ, Ringwald P, Silamut K, Imwong M, Chotivanich K, Lim P, Herdman T, An SS, Yeung S, Singhasivanon P, Day NP, Lindegardh N, Socheat D, White NJ. 2009. Artemisinin resistance in Plasmodium falciparum malaria. N Engl J Med 361:455-67.
6. Lu F, Culleton R, Zhang M, Ramaprasad A, von Seidlein L, Zhou H, Zhu G, Tang J, Liu Y, Wang W, Cao Y, Xu S, Gu Y, Li J, Zhang C, Gao Q, Menard D, Pain A, Yang H, Zhang Q, Cao J. 2017. Emergence of Indigenous Artemisinin-Resistant Plasmodium falciparum in Africa. N Engl J Med 376:991-3.
7. Gardner MJ, Hall N, Fung E, White O, Berriman M, Hyman RW, Carlton JM, Pain A, Nelson KE, Bowman S, Paulsen IT, James K, Eisen JA, Rutherford K, Salzberg SL, Craig A, Kyes S, Chan M-S, Nene V, Shallom SJ, Suh B, Peterson J, Angiuoli S, Pertea M, Allen J, Selengut J, Haft D, Mather MW, Vaidya AB, Martin DMA, Fairlamb AH, Fraunholz MJ, Roos DS, Ralph SA, McFadden GI, Cummings LM, Subramanian GM, Mungall C, Venter JC, Carucci DJ, Hoffman SL, Newbold C, Davis RW, Fraser CM, Barrell B. 2002. Genome sequence of the human malaria parasite Plasmodium falciparum. Nature 419:10.1038/nature01097.
8. Lin D, Yin X, Wang X, Zhou P, Guo F-B. 2013. Re-Annotation of Protein-Coding Genes in the Genome of Saccharomyces cerevisiae Based on Support Vector Machines. PLOS ONE 8:e64477.

9. Allman EL, Painter HJ, Samra J, Carrasquilla M, Llinas M. 2016. Metabolomic Profiling of the Malaria Box Reveals Antimalarial Target Pathways. Antimicrob Agents Chemother 60:6635-6649.
10. Cobbold SA, Chua HH, Nijagal B, Creek DJ, Ralph SA, McConville MJ. 2016. Metabolic Dysregulation Induced in Plasmodium falciparum by Dihydroartemisinin and Other Front-Line Antimalarial Drugs. J Infect Dis 213:276-86.
11. Creek DJ, Chua HH, Cobbold SA, Nijagal B, MacRae JI, Dickerman BK, Gilson PR, Ralph SA, McConville MJ. 2016. Metabolomics-Based Screening of the Malaria Box Reveals both Novel and Established Mechanisms of Action. Antimicrob Agents Chemother 60:6650-6663.
12. Olszewski KL, Morrisey JM, Wilinski D, Burns JM, Vaidya AB, Rabinowitz JD, Llinas M. 2009. Host-parasite interactions revealed by Plasmodium falciparum metabolomics. Cell Host Microbe 5:191-9.
13. Park YH, Shi YP, Liang B, Medriano CA, Jeon YH, Torres E, Uppal K, Slutsker L, Jones DP. 2015. High-resolution metabolomics to discover potential parasite-specific biomarkers in a Plasmodium falciparum erythrocytic stage culture system. Malar J 14:122.
14. Siddiqui RA, Williams JF. 1989. The regulation of fatty acid and branched-chain amino acid oxidation in cancer cachectic rats: a proposed role for a cytokine, eicosanoid, and hormone trilogy. Biochem Med Metab Biol 42.
15. Teng R, Lehane AM, Winterberg M, Shafik SH, Summers RL, Martin RE, van Schalkwyk DA, Junankar PR, Kirk K. 2014. 1H-NMR metabolite profiles of different strains of Plasmodium falciparum. Biosci Rep 34:e00150.
16. Parvazi S, Sadeghi S, Azadi M, Mohammadi M, Arjmand M, Vahabi F, Sadeghzadeh S, Zamani Z. 2016. The Effect of Aqueous Extract of Cinnamon on the Metabolome of Plasmodium falciparum Using (1)HNMR Spectroscopy. Journal of Tropical Medicine 2016:3174841.
17. Babbitt SE, Altenhofen L, Cobbold SA, Istvan ES, Fennell C, Doerig C, Llinas M, Goldberg DE. 2012. Plasmodium falciparum responds to amino acid starvation by entering into a hibernatory state. Proc Natl Acad Sci U S A 109:E3278-87.
18. Siddiqui G, Srivastava A, Russell AS, Creek DJ. 2017. Multi-omics Based Identification of Specific Biochemical Changes Associated With PfKelch13-Mutant Artemisinin-Resistant Plasmodium falciparum. J Infect Dis 215:1435-1444.
19. Ribaut C, Berry A, Chevalley S, Reybier K, Morlais I, Parzy D, Nepveu F, Benoit-Vical F, Valentin A. 2008. Concentration and purification by magnetic separation of the erythrocytic stages of all human Plasmodium species. Malar J 7:45.
20. Codd A, Teuscher F, Kyle DE, Cheng Q, Gatton ML. 2011. Artemisinin-induced parasite dormancy: a plausible mechanism for treatment failure. Malar J 10:56.
21. Carey MA, Covelli V, Brown A, Medlock GL, Haaren M, Cooper JG, Papin JA, Guler JL. 2018. Influential Parameters for the Analysis of Intracellular Parasite Metabolomics. mSphere 3.
22. Jackson KE, Spielmann T, Hanssen E, Adisa A, Separovic F, Dixon MW, Trenholme KR, Hawthorne PL, Gardiner DL, Gilberger T, Tilley L. 2007. Selective permeabilization of the host

cell membrane of Plasmodium falciparum-infected red blood cells with streptolysin O and equinatoxin II. Biochem J 403:167-75.
23. Peatey CL, Chavchich M, Chen N, Gresty KJ, Gray KA, Gatton ML, Waters NC, Cheng Q. 2015. Mitochondrial Membrane Potential in a Small Subset of Artemisinin-Induced Dormant Plasmodium falciparum Parasites In Vitro. J Infect Dis 212:426-34.
24. Teuscher F, Gatton ML, Chen N, Peters J, Kyle DE, Cheng Q. 2010. Artemisinin-induced dormancy in plasmodium falciparum: duration, recovery rates, and implications in treatment failure. J Infect Dis 202:1362-8.
25. Breglio KF, Rahman RS, Sa JM, Roberts DJ, Wellems TE. 2018. Kelch Mutations in Plasmodium falciparum Protein K13 Do Not Modulate Dormancy after Artemisinin Exposure and Sorbitol Selection In Vitro. Antimicrob Agents Chemother 62.
26. Trager W, Jensen JB. 1976. Human malaria parasites in continuous culture. Science 193:673-5.
27. Bei AK, Desimone TM, Badiane AS, Ahouidi AD, Dieye T, Ndiaye D, Sarr O, Ndir O, Mboup S, Duraisingh MT. 2010. A flow cytometry-based assay for measuring invasion of red blood cells by Plasmodium falciparum. Am J Hematol 85:234-7.
28. Lambros C, Vanderberg JP. 1979. Synchronization of Plasmodium falciparum erythrocytic stages in culture. J Parasitol 65:418-20.
29. Grimberg BT, Jaworska MM, Hough LB, Zimmerman PA, Phillips JG. 2009. Addressing the malaria drug resistance challenge using flow cytometry to discover new antimalarials. Bioorganic & medicinal chemistry letters 19:5452-5457.